# REPORT DOCUMENTATION PAGE

Form Approved
OMB NO. 0704-0188



1. AGENCY USE ONLY ( Leave Blank)

2. REPORT DATE 4-20-01

3. REPORT TYPE AND DATES COVERED
Final Report 01 Mar 97 - 28 Feb 01

4. TITLE AND SUBTITLE
Crack Tip Fields Mapping and Failure Characterization of Functionally Graded ~~Functionally Graded~~ Compositions

5. FUNDING NUMBERS
Grant # DAAG55-97-0110
~~Proposal # P-34908-EG~~

6. AUTHOR(S)
Hareesh V. Tippur

7. PERFORMING ORGANIZATION NAME(S) AND ADDRESS(ES)
Department of Mechanical Engineering
Auburn University
202 Ross Hall, Auburn, AL 36849

8. PERFORMING ORGANIZATION REPORT NUMBER



9. SPONSORING / MONITORING AGENCY NAME(S) AND ADDRESS(ES)
U. S. Army Research Office
P.O. Box 12211
Research Triangle Park, NC 27709-2211

10. SPONSORING / MONITORING AGENCY REPORT NUMBER
ARO 34908.9-EG

11. SUPPLEMENTARY NOTES
The views, opinions and/or findings contained in this report are those of the author(s) and should not be construed as an official Department of the Army position, policy or decision, unless so designated by other documentation.

12 a. DISTRIBUTION / AVAILABILITY STATEMENT
Approved for public release; distribution unlimited.

12 b. DISTRIBUTION CODE

13. ABSTRACT (Maximum 200 words)

Crack tip deformations and fracture parameters in functionally graded glass-filled epoxy beams are experimentally evaluated under static and dynamic loading conditions. Beams with unidirectional, monotonic elastic gradients and cracks along the gradient are examined. SEN samples with increasing or decreasing Young's modulus ahead of the crack tip are studied in symmetric four-point bending and one-point impact loading configurations. Optical method of Coherent Gradient Sensing (CGS) is used to measure crack tip deformations prior to crack initiation. For impact loading experiments, CGS is used in conjunction with high-speed photography for recording instantaneous deformation fields. Stress intensity factors (SIF) or SIF-histories in functionally graded materials (FGM) based on locally homogeneous material descriptions in the immediate crack tip vicinity are evaluated and compared with companion finite element simulations. The influence of elastic gradients in FGM samples with cracks on the compliant and stiff sides of the beam are quantified relative to their homogeneous counterparts and with each other. Under static loading conditions, the crack tip located on the compliant side of the beam is elastically shielded when compared to the situation when the crack is on the stiffer side of the same FGM beam. Under dynamic conditions, however, elastic gradients affect crack initiation differently. Crack initiation in an FGM with a crack on the stiff side of the beam and impact occurring on the compliant edge is delayed when compared to the opposite configuration. Independent finite element simulations of FGMs with idealized elastic gradients with identical crack tip elastic properties suggest that lower crack tip loading rate in the former is responsible for the differences.

14. SUBJECT TERMS

15. NUMBER OF PAGES
32

16. PRICE CODE

| 17. SECURITY CLASSIFICATION OR REPORT | 18. SECURITY CLASSIFICATION ON THIS PAGE | 19. SECURITY CLASSIFICATION OF ABSTRACT | 20. LIMITATION OF ABSTRACT |
|---|---|---|---|
| UNCLASSIFIED | UNCLASSIFIED | UNCLASSIFIED | UL |

**REPORT DOCUMENTAION PAGE (SF 298)**

FINAL REPORT

**ATTN:** Research Grant # DAAG55-97-0110
AMSRL-RO-RI 34909-EG

# CRACK TIP FIELD MAPPING AND FAILURE CHARACTERIZATION OF FUNCTIONALLY GRADED COMPOSTES

PI-PD: Hareesh V. Tippur
Department of Mechanical Engineering
Auburn University, 202 Ross Hall
Auburn, Alabama 36849

Submitted to:
**Army Research Office**
Attn: Dr. Mohammed Zikry
Solid Mechanics Program
P.O. Box 12211
Research Triangle Park, NC 27709-2211

April 2001

## TABLE OF CONTENTS

## LIST OF ILLUSTRATIONS



## LIST OF TABLES

## STATEMENT OF THE PROBLEM STUDIED

Relatively few experimental works on the fracture mechanics of FGMs is reported to date. This has been primarily due to the limitations regarding processing of such materials at scales suitable for laboratory experimentation. In this report, development, elastic characterization followed by failure characterization of a compositionally graded glass-filled epoxy particulate composite is presented. FGMs with cracks oriented along the direction of the elastic gradient are considered. Specifically, the influence of unidirectional elastic variations on crack initiation in FGMs subjected to static loading and low velocity impact is studied using optical interferometry, high-speed imaging and finite element techniques.

## SUMMARY OF RESULTS

Crack tip deformations and fracture parameters in functionally graded glass-filled epoxy beams are experimentally evaluated under static and dynamic loading conditions. Beams with unidirectional, monotonic elastic gradients and cracks along the gradient are examined. SEN samples with increasing or decreasing Young's modulus ahead of the crack tip are studied in symmetric four-point bending and one-point impact loading configurations. Optical method of Coherent Gradient Sensing (CGS) is used to measure crack tip deformations prior to crack initiation. For impact loading experiments, CGS is used in conjunction with high-speed photography for recording instantaneous deformation fields. Stress intensity factors (SIF) or SIF-histories in functionally graded materials (FGM) based on locally homogeneous material descriptions in the immediate crack tip vicinity are evaluated and compared with companion finite element simulations. The influence of elastic gradients in FGM samples with cracks on the compliant and stiff sides of the beam are quantified relative to their homogeneous counterparts and with each other. Under static loading conditions, the crack tip located on the compliant side of the beam is elastically shielded when compared to the situation when the crack is on the stiffer side of the same FGM beam. Under dynamic conditions, however, elastic gradients affect crack initiation differently. Crack initiation in an FGM with a crack on the stiff side of the beam and impact occurring on the compliant edge is delayed when compared to the opposite configuration. Independent finite element simulations of FGMs with idealized elastic gradients with identical crack tip elastic properties suggest that lower crack tip loading rate in the former is responsible for the differences.

## TECHNICAL DESCRIPTION AND ACCOMPLISHMENTS

### INTRODUCTION

Nonhomogeneous material systems with gradual variation in properties are collectively referred to as functionally graded materials or FGMs. Gradual variation of material properties in FGMs, unlike abrupt changes encountered in discretely layered systems, is known to improve failure performance (Niino, et. al., 1987) while preserving the intended thermal, tribological, and/or structural benefits of combining dissimilar materials. Accordingly, FGMs are considered ideal for applications involving high strain rate and thermal shock loading. Assessing the influence of compositional and hence material property gradients on the failure behavior is central for understanding FGMs. In this article, the influence of elastic gradients on the static and dynamic crack initiation in FGMs is examined. *Of specific interest to this work are FGMs with cracks parallel to the elastic gradient.*

Some of the early works on the fracture mechanics of FGMs include those by Atkinson and List (1978), and Delale and Erdogan (1983). An inverse $\sqrt{r}$ stress singularity at the crack in FGMs was suggested in these articles and was later confirmed by Eischen (1987) using asymptotic analysis. Jin and Noda (1994) concluded likewise, independently of the crack orientation relative to the property gradient. In a paper summarizing recent advances in fracture mechanics of FGMs, Erdogan (1995) has presented theoretical results for cracks oriented along the elastic gradient, and subjected to various loading conditions. Among the dynamic investigations on FGMs, transient stress intensity factors for a mode-III crack lying in an elastic media with spatially varying elastic properties normal to crack surfaces has been studied analytically by Babaei and Lukasiewicz (1998). They have found SIF to vary with crack length to layer thickness ratio. Dynamic crack propagation in functionally graded particulate is numerically studied by Nakagaki et al., (1998) for shock loading to determine the effect of grading on crack severity as the crack propagates in the FGM. Parameswaran and Shukla (1998) have shown experimentally that increasing toughness in the direction of crack growth reduces crack jump distance in discretely layered FGMs. Chiu and Erdogan (1999) have evaluated the effect of material nonhomogeneity on one-dimensional wave propagation in FGMs having gradation in the direction of the incident pulse. Considerable wave distortions are reported as a

rectangular pressure pulse propagates in the material. Parameswaran and Shukla (1999) have performed asymptotic analysis to establish equations describing stress fields around steadily growing cracks along the elastic gradient of FGMs. They have obtained explicit expressions for sum of in-plane normal stresses and nonhomogeneity specific higher order terms.

## ELASTIC CRACK TIP FIELDS IN FGMS: BACKGROUND

Stationary Crack: For a crack oriented along the direction of the elastic gradient in a nonhomogeneous, isotropic planar body, using asymptotic analysis, Eischen (1987) has shown that the crack tip stresses, say $(\sigma_x + \sigma_y)$, in an FGM for mode-I conditions can be expressed as,

$$(\sigma_x + \sigma_y) = \left( C_0 r^{-\frac{1}{2}} f_0^I(\theta) + C_1 r^0 f_1^I(\theta) \right) + O\left( r^{\frac{1}{2}} \right), \tag{1}$$

where $(r, \theta)$ denote crack tip polar coordinates, $f_0^I, f_1^I$ are angular functions, and $C_0$ and $C_1$, are the coefficients of the expansion with $C_0 = \frac{K_I}{\sqrt{2\pi}}$, $K_I$ being the mode-I stress intensity factor. The angular functions have been shown to be identical to the ones for a crack in a homogeneous body. Accordingly, stress field description is identical to the homogeneous counterpart for the first two terms of the expansion. Expressions for in-plane displacements in FGMs were also developed by Eischen (1987). It was found that asymptotic displacement terms proportional to $r^{1/2}$, $r^0$, and $r^1$ are identical to those of homogeneous materials, thus are independent of gradient. The experimental method used in the current study measures surface slopes, and hence expressions for out-of-plane displacements, $w$, are necessary. Assuming plane stress conditions and constant thickness-wise strain, out-of-plane displacement can be obtained as,

$$w \approx \frac{-\nu B}{2} \left( A_0 r^{-\frac{1}{2}} f_0^I(\theta) + A_1 r^0 f_1^I(\theta) + A_2 r^{\frac{1}{2}} f_2^I(\theta) \right) + O(r), \tag{2}$$

with $A_j = C_j / E_0$ where the subscript $E_0$ denotes the value of crack tip Young's modulus. In the above, the Poisson's ratio $\nu$ is assumed to be constant in the FGM.

Near tip expressions for stress fields in nonhomogeneous planar bodies that include the influence of elastic property gradients are reported by Erdogan, (1995). For an exponential variation of elastic modulus of the form,

$$E(x) = E_0 e^{\alpha x} = E_0 e^{r\alpha\cos\theta}, \tag{3}$$

where $E_0$ is the Young's modulus at the origin, and $\alpha$ is a scalar dependent on the terminal values of the modulus and the length of the graded region, the near tip mode-I stresses are shown to be of the form,

$$\sigma_{ij}(r,\theta) \cong e^{r\alpha\cos\theta}\left(\frac{K_I}{\sqrt{2\pi r}} f_{ij}^{I}(\theta)\right), \qquad (i,j = x,y). \tag{4}$$

As $r \to 0$, eq. (4) reduces to the K-dominant terms of eq. (2).

In the absence of explicit expressions for stress fields for dynamically loaded stationary cracks, it could be inferred that eq. (2) could be adequately extended for dynamic cases where inertial effects enter the coefficients without modifying the overall form of the expressions (i.e., $A_i \equiv A_i(t)$).

Dynamically Propagating Crack: At the moment, analytical work on dynamically propagating cracks in FGMs has been very limited. To authors' knowledge, only Parameswaran and Shukla (1999) have reported crack tip stress fields near dynamically propagating cracks in FGMs. Explicit expressions for stress quantity $(\sigma_x + \sigma_y)$ for mode-I and –II situations are provided for steadily propagating cracks along the gradient with linearly or exponentially varying shear moduli. The solutions correspond respectively to specialized cases where constant density ($\rho$) with varying Young's modulus ($E$) is assumed or constant $E/\rho$ ratio is assumed.

## EXPERIMENTS

*The Material Processing and Elastic Characteristics*

Compositionally graded samples used in the current research comprised of an epoxy matrix (Young's modulus ~ 3 GPa, Poisson's ratio ~ 0.35) in which varying quantities of solid A-glass spheres (mean diameter ~ 42 μm) were dispersed to achieve elastic property variations at macroscopic scales. Thus the composite is *microscopically heterogeneous* but will be treated as an *isotropic, non-homogeneous material at macroscopic scales* for measurement and analysis using continuum models.

Prior to discussing the material properties of the FGMs used in the experiments, properties of homogeneous particulate glass-epoxy composites with different volume fraction of filler are described. Figure 1(a) shows measured Young's modulus and Poisson's ratio variation of macroscopically *homogeneous mixtures* having different but constant volume fractions of the filler in the matrix. Young's modulus from about 3 to 9 GPa (static conditions) and a Poisson's ratio variation from 0.35 to 0.29 when the volume fraction of the filler is increased from zero to 0.5. Also included in the figure are micromechanics predictions of the elastic modulus for two-phase mixtures (Weng, 1984) for different volume fractions $V_f$. Evidently, the predictions follow the experimental measurements rather closely over the entire range of filler volume fractions. (It should also be noted that these particle filled compositions show a linear load-displacement behavior (Butcher, et al., 1999) and can be treated to be nominally linear elastic). In Fig. 1(b), the dynamic material properties namely longitudinal and shear wave speeds and density of the composites are shown. Evidently, each of these properties increases monotonically with the filler volume fraction in the composite.

Gravity casting was used for producing FGMs with monotonic Young's modulus variation between approximately 3 and 9 GPa under static conditions (measured using cantilever beam tests) or, approximately 4 to 12 GPa, under dynamic conditions (measured using ultrasonic pulse-echo measurements). These values of Young's moduli correspond to that of pure epoxy and a composite with a volume fraction of glass spheres in an epoxy matrix of $\sim$ 0.5, respectively. Details of the methods used in determining the elastic characteristics can be found in Butcher, et al., (1999). Figure 2 shows the modulus variation in a typical FGM sheet. The graded region in these sheets were machined into beam samples (dimensions 120 mm x 20 mm x 6 mm for static experiments and 150 mm x 37 mm x 6 mm for dynamic experiments). Figure 2 shows typical elastic variation in a casting of which a portion was machined to obtain beam samples having the necessary elastic properties. The sample surfaces were then deposited with a thin layer of aluminum to obtain specular surface necessary for optical measurements. Edge notches (root radius 75 μm and length of 6 mm) were cut into the samples using a high-speed diamond impregnated circular saw.

Homogeneous samples (without compositional gradients) having elastic moduli equal to the ones at the crack tips of the FGMs were also prepared for comparative study. The geometry of these homogeneous samples was identical to that of the FGM samples.

*Optical Technique: Coherent Gradient Sensing*

The optical method of *reflection* Coherent Gradient Sensing (CGS) was used for measuring crack tip deformations. The working principle of CGS has been reported by Tippur, et al., (1991). An expanded and collimated beam of laser light (typically 50 mm in diameter) was used to interrogate the *specular* surface of the specimen. The reflected light beam, or the object wave front, contained information about the surface deformations. Optical shearing of the object wave front was used to decipher surface deformations in the form of interference patterns representing contours of constant surface slopes. In the present work, surface slopes along the crack orientation ($x$-axis) were determined as,

$$\frac{\partial w}{\partial x} = \frac{Np}{2\Delta}, \qquad N = 0, \pm 1, \pm 2, \ldots, \tag{5}$$

where $N$ denotes fringe orders, $p$ is the pitch of the gratings (25 μm), and $\Delta$ is the grating separation distance. For plane stress conditions, the out-of-plane displacement $w$ can be related to the in-plane stress components using expression for average out-of-plane strain, $\varepsilon_z \cong \frac{2w}{B}$, or,

$$w \cong -\frac{\nu B}{2}\left(\frac{\sigma_x + \sigma_y}{E}\right), \tag{6}$$

where $B$ is the undeformed thickness of the sample.

Interference fringes were recorded in real-time using a conventional camera during static experiments. The experimental set-up for dynamic study, however, was more elaborate. It included an impactor for stress wave loading, a pulse-laser as a light source, a CGS interferometer and a continuous access high-speed camera. During the experiment, a pneumatically operated impactor with a steel cylindrical head was launched towards the specimen. During its descent, the hammer first triggered open an electronic shutter of the high speed rotating mirror camera pre-spun to the desired speed, allowing light to reach its internal cavity. The specimen was subjected to one point symmetric impact. An adhesive-backed copper

tape placed on the top edge of the beam closed an electric circuit when contacted by the hammer. This in turn triggered the laser to begin pulsing at a repetition rate of 5 μs, with a pulse width of 50 ns, for a time duration of less than or equal to a single sweep of the light beam on the stationary film track of the high-speed camera.

*Optical Measurements*

Statically Loaded Stationary Cracks: The FGM and homogeneous beam samples were quasi-statically loaded in four-point bending using an Instron-4465 machine in displacement control mode (cross-head speed ~ 0.25 mm per minute). The samples were subjected to symmetric bending moment acting over a 60 mm length in the mid-span of each beam. The resulting crack tip fringe patterns in FGMs with a crack on the stiff ($E_2 / E_1 < 1$) and the compliant sides ($E_2 / E_1 > 1$) of the beam are shown in Figs. 3(a) and 3(c), respectively. In these cases, the crack tip Young's moduli were 6.8 GPa and 4.8 GPa, respectively. Further, the far-field applied stress $\sigma_\infty$ ($= 6M / BW^2$, where $M$ is the moment, $W$ and $B$ are the beam height and thickness, respectively) at which the deformations were recorded in the two cases are the same. Homogeneous samples having crack tip Young's moduli same as (to within ± 3%) that of the FGMs were also optically investigated. The crack-tip deformation patterns for the homogeneous beams corresponding to the FGMs with the crack on the stiff and compliant side are shown in Fig. 3(b) and 3(d), respectively. Note that, the fringe patterns from the homogeneous samples are for the same load level as their FGM counterparts. The sensitivity of the optical measurements is ~ 0.015° / fringe. In each case, the fringes are nominally symmetric about the crack plane indicating mode-I behavior. However, qualitative differences exist between the fringe patterns in terms of relative fringe sizes between front and rear crack tip lobes in FGMs and, between the ones in FGMs and the equivalent homogeneous beams. These differences were quantified by extracting crack tip stress intensity factors from the fringe patterns.

Dynamically Loaded Stationary Cracks: The FGM and homogeneous beam samples were impact loaded in one-point symmetric loading configuration with a velocity of 5.3 m/s. The resulting interference patterns representing contours of $dw / dx$ were recorded at a rate of 200,000 frames per second. For brevity, two select interferograms are shown for each experiment, at times 25 μs and 75 μs after impact, the latter being close to crack initiation in each case. CGS fringes for the

homogeneous material are shown in the first column of Fig. 4. Fringes for the FGMs with crack located on compliant and stiff sides of the gradient are shown in the second and third columns of Fig. 4, respectively. The homogeneous beam had a uniform volume fraction of 0.42, and an elastic modulus of 9.6 GPa. The FGM with crack on the compliant side ($E_2 / E_1 \sim 2.9$) has elastic modulus variation between 4 and 11 GPa with a value of $E_o \sim 5.6$ GPa at the crack tip. Terminal values of Young's moduli are nearly the same for the FGM with crack on the stiff side ($E_2 / E_1 \sim 0.45$), with crack tip $E_o \sim 10$ GPa.

The structure of the fringe patterns in the crack tip vicinity for the two FGMs qualitatively resemble those in the homogeneous material. At the crack tip, one set of frontal and two sets of equally prominent lateral fringe lobes are present. Further examination of crack tip fringes in the FGM with crack on the compliant side ($E_2 / E_1 > 1$, Fig. 4) show some deviation relative to the homogeneous case. Crack tip fringe lobes ahead of the crack show a lateral spread normal to impact direction. In this case, the compressive stress waves progressively slow down as they encounter more compliant material when they propagate away from the stiff edge. The opposite occurs when the tensile waves are reflected from the cracked edge. Crack tip fringes for the FGM with crack on the stiff side ($E_2 / E_1 < 1$, Fig. 4) have a similar appearance to those for the homogeneous material. Here, the compressive stress waves generated at the compliant edge progressively encounter stiffer material and hence speed up during propagation away from the compliant edge. Nearly equi-sized front and rear fringe lobes around the crack tip are present. Additionally, a relatively uniform far-field is evident in this specimen.

For the homogeneous sample ($E_2 / E_1 = 1$) with a longitudinal velocity of ~ 2980 m/s, approximately 12.5 μs are required for the initial compressive waves to reach the bottom edge of the beam. The reflected tensile waves load the crack tip ~ 15 μs after impact. Following that, crack tip fringes progressively enlarge and become more numerous up to crack initiation at ~ 85 μs. Average longitudinal wave speed $\left( \bar{C}_l = \frac{1}{W} \int_{-a}^{W-a} C_l(x)\,dx \right)$ for the FGM specimen with crack on the compliant side ($E_2 / E_1 > 1$) is ~ 2910 m/s. In this case, initial propagation times of compressive and reflected tensile waves are similar to those of the homogeneous material. It is important to remember here that compressive waves progressively slow down as the crack tip is

approached while the opposite is true for reflected tensile waves. The crack initiates ~ 80 μs after impact. The FGM with the crack on the stiff side ($E_2 / E_1 < 1$) has an average longitudinal velocity of ~ 2900 m/s over the height of the beam. Again, this velocity corresponds to times of ~ 12.5 μs for a compressive wave to reach the bottom edge, and ~ 2.5 μs for a tensile wave to reflect to the crack tip. In this case, the incoming compressive waves from the contact point travel progressively faster towards the crack tip while the reverse occurs for the reflected tensile waves. The size of the crack tip fringes increases gradually until initiation at about 90 μs. An observation pertinent to FGM and homogeneous specimens can be made: compressive and tensile waves arrive at the original crack tips at approximately the same times for all the specimens since the average longitudinal wave speeds are nearly same. Therefore, initial crack tip loading occurs at nearly the same time. Local properties at individual crack tips, as well as non-uniform wave reflections from the edges will contribute to varying conditions in crack initiation between the different specimens. Evidently, the crack in the FGM with $E_2 / E_1 < 1$ experiences delayed crack initiation relative to the one with $E_2 / E_1 > 1$.

Extraction of Stress Intensity Factors from Interferograms: Overdeterministic least-squares analyses of optical data (Tippur, et al., 1991) were used for extracting instantaneous stress intensity factors. Briefly, the method consisted of digitizing the interferograms around the crack tip to obtain fringe order $N$ and location $(r, \theta)$ data. In view of 3-D effects in the immediate crack tip vicinity, optical data within $r/B < 0.4$ were not considered in the analysis. This was based on existing knowledge of crack tip field triaxiality in finite size homogeneous samples (Rosakis and Ravichandar, 1987). Further, for mode-I, it has been shown using CGS that (Tippur, et al., 1991), data in the sector $90^\circ < |\theta| < 135^\circ$ have the least amount of 3-D effects and closely follow plane stress behavior. (Similar conclusions have been drawn in case of bimaterial interfacial cracks in finite thickness samples as well (Sinha and Tipur, 1997).) Also, a difference representation of eq. (5) was used for least-squares data analysis, by minimizing the least-squares error $\left(\frac{\delta w}{\delta x} - \frac{Np}{2\Delta}\right)^2$ ($w$ as given in the right hand side of eq. (2)) at all digitized data points with respect to the unknown coefficients $A_0$ ($\propto K_{Id}$), $A_1$, and $A_2$, the stress intensity factor was evaluated.

## NUMERICAL SIMULATIONS

*Elasto-Static Computations*

Companion finite element simulations of cracked FGM samples were carried out. *Plane stress* elasto-static simulations of cracked beams subjected to pure bending were performed for both FGMs and homogeneous materials. Owing to the symmetry, only one half of the beam was modeled with appropriate force and displacement boundary conditions. In the case of FGM beams, measured Young's modulus gradient from the samples was prescribed for FGMs using a novel technique developed by Rousseau and Tippur (2000). The Poisson's ratio was assumed constant and equal to a value corresponding to that of the crack tip, throughout the model. Separate simulations were carried out for situations with crack located on the stiff and the compliant sides of FGM beams. The corresponding crack tip elastic properties were used in separate homogeneous beam simulations. A typical model consisted of 8600 eight-noded isoparametric elements with 26000 nodes and two degrees of freedom per node, as shown in Fig. 5. The crack tip region had a square mesh with a typical size of 50-100 μm.

In the immediate vicinity of the crack tip, assuming K-dominance, the expressions for crack opening displacements were truncated to the leading term and used for determining stress intensity factors in FGMs in the limit $r \rightarrow 0$. Thus, for a locally homogeneous material behavior, crack opening displacement for an FGM is,

$$\delta_y(t)|_{\theta=\pm\pi, r\to 0} = \frac{8\bar{K}_I(t)}{E_0}\sqrt{\frac{r}{2\pi}}. \tag{7}$$

Here, $E_o$ is the crack tip Young's modulus. The variation of $\bar{K}_I(r, \pm\pi)$ obtained from the finite element solution was first plotted and its extrapolated value at the crack tip was identified as the stress intensity factor:

$$K_I = \lim_{r\to 0} \bar{K}_I. \tag{8}$$

*Elasto-Dynamic Computations*

Companion *plane stress* elasto-dynamic finite element simulation of all the three categories of experiments, homogeneous and the two FGMs, were performed. A two-

dimensional quadrilateral mesh of eight-noded isoparametric elements with two degrees of freedom per node was used in the analysis. Again because of the symmetry, only one half of each sample was modeled, with approximately 10000 nodes and 3300 elements. The crack tip vicinity was highly refined as in static simulations for accurate evaluation of crack tip parameters. Simulations were conducted as a one point symmetric impact of an elastic planar medium by a rigid impactor, by imposing the downward velocity of 5.3 m/s (equal to the impact velocity of the experiments) to the topmost node in the plane of the crack. The Newmark time-integration scheme was used with a minimum time step of 0.04 μs. As in the static simulations, instantaneous mode-I stress intensity factors were determined by regression analysis of crack tip opening displacements at discrete time intervals of every 5 μs after impact until crack initiation.

## RESULTS AND DISCUSSION

*Static Loading*

FGM specimens were subjected to far-field bending stress ($6M / BW^2$) of 10.2 MPa. The FGM sample with a crack located on its compliant side had a crack tip modulus $E_0$ = 4.8 GPa, and a modulus ratio ($E_2 / E_1$) between its two edges of 2.2. The other FGM sample, with an edge crack on the stiff side had a crack tip modulus $E_0$ = 6.8 GPa, and a modulus ratio of 0.4. The homogeneous samples with moduli corresponding to those at the crack tips ($E_0$) of the FGMs were subjected to far-field stresses identical to those of their FGM counterparts, so that a direct comparison could be made.

A comparison of the mode-I stress intensity factors obtained from the analysis of interferograms is presented in Table 1. Under the premise of $K$-dominance, the experimental values of $K_I$ for the FGMs are about 20 % lower than those predicted by the finite element calculations. When least-squares analysis including non-singular contributions to the singular field was carried out with two terms of the expansion field (eq. (5)), the values of stress intensity factors improved and the error between the numerical and experimental results reduced to 10 % or less.

The influence of elastic gradient on statically loaded FGM beams can be inferred from stress intensity factor results. The beam with a crack on the glass-rich (stiff) side ($E_2 / E_1 < 1$)

experience higher value of $K_I$ when compared to its homogeneous counterpart subjected to identical far-field loading. On the other hand, the FGM beam with a crack on the epoxy-rich (compliant) side ($E_2 / E_1 > 1$) of the beam experiences a lower $K_I$ compared to its homogeneous counterpart. Thus in the specific case studied, the results suggest that elastic gradients shield a crack on the compliant side and lower the stress intensity factor by a factor of about 1.5 when compared to the one with the crack on the stiff side.

*Dynamic Loading*

Instantaneous stress intensity factors, $K_{Id}(t)$, were evaluated up to crack initiation. Symbols in Fig. 6(a) and (b) represent optically determined dynamic stress factor history for the two FGMs with $E_2 / E_1 < 1$ and $E_2 / E_1 > 1$, respectively. Finite element results are also plotted as a solid line, up to crack initiation, $t_i$ (determined experimentally). Good agreement between the two is evident. Note the absence of experimental data points for certain frames because of either loss of optical information and/or, during early stages of fringe formation, the fringes reside within the region of dominant triaxiality where they can not be reliably analyzed.

For comparison purposes, normalized stress intensity factors are plotted against normalized time for the two FGMs and homogeneous sample in Fig. 6(c). In this, time after impact is normalized with respect to the dilatational wave speed at the crack tip location and the specimen height: $T = t * C_l / W$ and stress intensity factors are normalized by the corresponding value at initiation. In each case, monotonic increase in $K_{Id}(t)$ is observed. Crack initiation occurred at $T \sim 6.8$ after initiation for the homogeneous material. Evidence of crack motion was not observed until $T \sim 6.2$ and 7.2 for the FGMs with $E_2 / E_1 > 1$ and $E_2 / E_1 < 1$, respectively. Note that the behavior of the homogeneous material lies between those of the two FGMs. Interestingly, crack initiation in FGMs with $E_2 / E_1 < 1$ are delayed relative to the opposite FGM configuration and the homogeneous sample. Also, evident from the plots are the differences in the crack tip loading rate ($\Delta K_{Id} / \Delta t$) with lower rate seen in case of the FGM with the crack on the stiff side of the beam.

In the results discussed above, in addition to the local fracture toughness difference at the crack tips, it should be noted that crack initiation event is affected by combination of differences

in the average values of wave speeds, crack tip elastic modulus and crack tip elastic gradients ($d(E/\rho)/dX$) between samples. Accordingly finite element simulations were carried out to isolate the effect of elastic gradients on crack initiation. Homogeneous beams and FGM beams with assumed linear elastic variations were simulated. Further, material variations were identified in terms of $E/\rho$ variations and Poisson's ratio was kept constant ($\nu = 0.34$). Material properties implemented were close to those realized in the actual glass/epoxy FGMs used in the experiments. The Young's moduli were varied between 4 GPa and 12 GPa, and densities between 950 kg/m$^3$ and 1850 kg/m$^3$. Individual variations of $E$ and $\rho$ were implemented using a 'look-up' chart relating $E$, $\rho$, (and $E/\rho$) to filler volume fraction in actual glass-filled epoxy. The prescribed elastic gradients consisted of linearly increasing and decreasing values of $E/\rho$ for FGMs, and constant $E/\rho$ representing homogeneous materials, all having identical properties at he crack tip (Fig. 7(a)). By selecting an $a/W = 0.5$, the crack tip Young's moduli, average value of the elastic wave speeds and $|d(E/\rho)/dX|$ were identical in all three situations. Thus, the influence of increasing and decreasing elastic gradients could be isolated.

Plot of $K_{Id}$ history after impact is shown in Fig. 7(b) for the three cases. The variation in stress intensity factor for the FGM with $E_2/E_1 > 1$ displays the highest rate of increase whereas the FGM with $E_2/E_1 < 1$ has the lowest rate of increase. The homogeneous material response lies in between the two FGMs. Rates of increase in $dK_{Id}/dt$ (Fig. 7(c)) are also lowest for FGM with $E_2/E_1 < 1$, followed by the homogeneous material. The FGM with $E_2/E_1 > 1$ has the steepest increase up to $T \sim 5$. Beyond that point, an inflection in the curve drops the increase in stress intensification below that of the homogeneous material but still higher than that for FGM with $E_2/E_1 < 1$. Material properties at the crack tip being the same in all the three cases, for an *assumed* critical value of stress intensity factor of, say, 3 MPa-$\sqrt{m}$, crack initiation occurs (Fig. 7(b)) at $T \sim 5.8$, 6.6, and 7.9 for FGM with increasing gradient, homogeneous material, and FGM with decreasing gradient, respectively. These trends are identical to the ones observed experimentally. Thus, purely based on elastic considerations, crack initiation in the latter case is significantly delayed, by a factor of ~1.4, when compared to the former. Behavior of the homogeneous material, as with all other parameters, lies between the two FGMs.

To further understand these differences, additional dynamic impact simulations on *uncracked* beams (FGM and homogeneous) were performed for monitoring stress histories. Contours of $(\sigma_x + \sigma_y)$ for all three materials are shown in Fig. 8 after several wave reflections ($T$ = 5.7) between the top and bottom edges. Relative to the homogeneous beam (Fig. 8(b)), compressive waves emanating from the impact point for the FGM with $E_2 / E_1 > 1$ (Fig. 8(c)) are constricted vertically, whereas those for the FGM with $E_2 / E_1 < 1$ (Fig. 8(a)) are elongated in the same direction. In the former case, as compressive waves (for example, contour level D) travel from the top to the bottom edge, they are delayed by material property variations in that direction. Conversely, for the FGM with $E_2 / E_1 < 1$, material property variation promotes faster wave propagation downwards, thereby elongation of $(\sigma_x + \sigma_y)$ contour (again, level D) along the beam height is evident. The reflected tensile waves accelerate upward for FGMs with $E_2 / E_1 > 1$, decelerate for FGMs with $E_2 / E_1 < 1$, and propagate at a constant speed in the homogeneous case. As seen in Fig. 8, at time $T$ = 5.7, a point P (located at $X / W$ = 0.5) along the line of symmetry of the beam experiences tensile stresses for the FGM with $E_2 / E_1 > 1$ while the corresponding points in the homogeneous beam and the FGM beam with $E_2 / E_1 < 1$ experience progressively higher compressive stresses, respectively. Accordingly, the latter two cases are elastically shielded from tensile stresses for a longer duration and would experience delayed crack initiation.

## CONCLUSIONS

Influence of elastic variations on crack initiation in compositionally graded beams was studied experimentally and numerically. Beam samples with unidirectional elastic gradients subjected to static four-point bending and dynamic one-point impact loading were considered for experimentation. Compositionally graded epoxy with solid-microsphere glass filler was the material of choice for producing elastic gradients by continuously varying filler volume fractions over the height of the beam samples. Macroscopic Young's modulus variations of about 1:3 and density of about 1:2 were realized using gravity casting. The optical method CGS was used for measuring surface slopes in the direction of elastic gradients. The high-speed photography was utilized for dynamic crack initiation studies for capturing instantaneous deformation field histories. A locally homogeneous material behavior in the immediate vicinity of the FGM crack tip is assumed for extracting stress intensity factors in both static and dynamic situations using

continuum models for crack stresses. Companion plane stress finite element simulations for both static and dynamic loading situations were performed and SIFs were determined using regression analysis of crack tip opening displacements. The experimentally determined values of stress intensity factors are in good agreement with the ones from computations.

Under static loading conditions, the elastic gradients offer crack tip shielding. In the specific examples studied, the crack tip located on the compliant side of a beam subjected to pure bending moment experienced SIF 1.5 times lower than that with a crack on the stiff side in a beam with an identical elastic variation. In the dynamic experiments, crack initiation in situation when the crack is located on the stiffer side of the beam were delayed when compared to the opposite situation when the crack is located on the compliant. However, this was a combined effect of the crack tip variables such as elastic properties, elastic gradient and the local fracture toughness. Accordingly, computations on dynamically loaded stationary cracks were performed for idealized situations where identical crack tip elastic properties were enforced and the effect of elastic gradients alone was isolated. Results confirmed the experimental observation that crack initiation in an FGM with crack on the stiff side of a beam subjected to symmetric one-point impact is delayed considerably when compared to the opposite configuration due to lower rate of crack tip loading.

## RESULTING PUBLICATIONS

### Refereed Journal Articles – Published/Accepted

1. 'Dynamic Fracture of Compositionally Graded Materials with Cracks along the Elastic Gradient', Experiments and Analysis, C.-E. Rousseau* and H.V. Tippur, *Mechanics of Materials*, 2000, accepted.

2. Compositionally Graded Materials with Cracks Normal to the Elastic Gradient: Examination of Fracture Parameters Relative to Bimaterials', C.-E. Rousseau* and H.V. Tippur, *Acta Materialia*, 2000, Vol. 48, pp 4021-4033.

3. 'Dynamic response of bimaterial and graded interface cracks under impact loading', P.R. Marur* and H.V. Tippur, *International Journal of Fracture*, Vol. 103, pp 95-109, 2000.

4. 'A functionally graded particulate composite: Preparation, measurements and Failure analysis', R.J. Butcher*, C. -E. Rousseau* and H.V. Tippur, *Acta Materialia*, Vol. 47, No.1, pp 259-268, 1999.

5. 'Evaluation of Mechanical Properties of Functionally Graded Materials', by P. Marur* and H. V. Tippur, *ASTM Journal of Testing and Evaluation*, Vol. 26, No. 6, pp 539-545, 1998.

### Refereed Journal Articles - Submitted

1. 'Influence of Elastic Gradient Profiles on Dynamically Loaded Functionally Graded Materials: Cracks Along the Gradient', C.-E. Rousseau* and H.V. Tippur, submitted to *International Journal of Solids and Structures*, 2000.

2. 'Evaluation of Crack Tip Fields and Stress Intensity Factors in Functionally Graded Elastic Materials: Cracks Parallel to Elastic Gradient, C. -E. Rousseau* and H.V. Tippur, submitted to *International Journal of Fracture*, 2000.

### Full-Length Articles in Conference Proceedings

1. 'Evaluation of Dynamic Crack-Tip Fields and Fracture Parameters in Functionally Graded Materials', C.-E. Rousseau and H.V. Tippur, Proceedings of IX International Congress on Experimental Mechanics, Orlando, FL, June, 2000.

2. "Optical measurement of fracture parameters in functionally graded composite beams", C.E. Rousseau and H.V. Tippur, Proceedings of the 1999 SEM Spring Conference, pp 62-65, Cicinnati, OH.

3. 'Interferometric measurement of fracture parameters in functionally graded glass-epoxy composite', Proceedings of the 15$^{th}$ U.S. Army Symposium on Solid Mechanics, Myrtle Beach, SC, 1999, pp 141-153, Battelle Press.

**Conference Presentations**

1. 'Evaluation of Dynamic Fracture Parameters in Functionally Graded Material', presented at ICTAM-2000, (20th International Congress of Theoretical and Applied Mechanics), H.V. Tippur and C.-E. Rousseau, Chicago, IL, September, 2000. (invited)

2. 'Optical Measurement of Dynamic Crack Tip Fields and Fracture Parameters in Functionally Graded Materials' by H.V. Tippur and C. -E. Rousseau, presented at 1999 ASME – IMECHE, Nashville, TN, November, (invited).

3. 'Evaluation of crack tip parameters in functionally graded composites: An optical and numerical Investigation', H.V. Tipur and H.V. Tippur, presented at the 1999 ASME Summer Annual Conference, Blacksburgh, VA, Book of Abstracts, pp 75 (invited).

4. 'A Comparative Study of Bimaterial, homogeneous and functionally graded Fracture Behavior', C. -E. Rousseau and H.V. Tippur, presented at the IMECH&E, Anaheim, CA., Nov., 1998, AMD Vol. 229, pp 127.

5. 'Experimental and Numerical investigation of fracture parameters in a functionally graded material', R.J. Butcher*, C. -E. Rousseau* and H.V. Tippur, presented at the USNCAM13, June, 1998, Gainesville, FL.

6. "Crack tip measurements in a particulate functionally graded material: experimental and numerical simulations", R.J. Butcher* and H.V. Tippur, ASME IMECH&E, Atlanta, November, 1996.

**Technical Reports to ARO**

| | |
|---|---|
| Annual Progress Reports for the project: | December 1997 |
| | December 1998 |
| | December 1999 |
| | December 2000 |

**PARTICIPATING PERSONNEL – DEGREE EARNED**

- Prabhakar R. Marur, obtained **Ph.D.** in Mechanical Engineering at Auburn University, **1998**, while being *partially supported* by the project.

- Carl-E. Rousseau, obtained **Ph.D.** in Mechanical Engineering at Auburn University, **2000**. *(Dr. Rousseau is a minority student, U.S. Citizen).*

## BIBLIOGRAPHY


Atkinson, C., and List, R. D., 1978, "Steady State Crack Propagation into Media with Spatially Varying Elastic Properties." International Journal of Engineering Science, Vol. 16, pp. 717-730.

Babaei, R., and Lukasiewicz, S. A., 1998, "Dynamic Response of a Crack in a Functionally Graded Material Between Two Dissimilar Half-Planes under Anti-Plane Shear Impact Load." Engineering Fracture Mechanics, Vol. 60, No. 4, pp. 479-487.

Butcher, R. J., Rousseau, C.-E., and Tippur, H. V., 1999, "A Functionally Graded Particulate Composite: Preparation, Measurements and Failure Analysis." Acta Materialia, Vol. 47, No. 1, pp. 259-268.

Chiu, T. C., and Erdogan, F., 1999, "One-Dimensional Wave Propagation in a Functionally Graded Elastic Medium." Journal of Sound and Vibration, Vol. 222, pp. 453-487.

Delale, F., and Erdogan, F., 1983, "The Crack Problem for a Nonhomogeneous Plane." ASME Journal of Applied Mechanics, Vol. 50, pp. 609-614.

Eischen, J. W., 1987, "Fracture of Nonhomogeneous Materials." International Journal of Fracture, Vol. 34, pp. 3-22.

Erdogan, F. (1995), "Fracture Mechanics of Functionally Graded Materials." Composites Engineering, Vol. 7, pp. 753-770.

Jin, Z.-H., and Noda, N., 1994, "Crack-Tip Singular Fields in Nonhomogeneous Materials." ASME Journal of Applied Mechanics, Vol. 61, pp. 738-740.

Marur, P. R., and Tippur, H. V., 1998, "Evaluation of Mechanical Properties of Functionally Graded Materials." Journal of Testing and Evaluation, Vol. 26, pp. 539-545.

Marur, P. R., and Tippur, H. V., 2000, "Dynamic Response of Bimaterial and Graded Interface Cracks Under Impact Loading." International Journal of Fracture, Vol. 103, pp 103-109.

Nakagaki, M., Wu, Y. D., and Hagihara, S., 1998, "Dynamically Propagating Crack in Graded Particle Dispersed Composites." Fracture and Strength of Solids, Vol. 145, pp. 333-342.

Nino, M., Hirai, T., Watanabe, R., 1987, "The Functionally Gradient Materials." Journal of the Japan Society of Composite Materials, Vol. 13, pp. 257.

Parameswaran, V., and Shukla, A., 1999, "Crack-tip Stress Fields for Dynamic Fracture in Functionally Gradient Materials." Mechanics of Materials, Vol. 31, pp. 579-596.

Rosakis, A. J., and Ravi-Chandar, K., 1986. "On Crack-Tip Stress State: An Experimental Evaluation of Three-Dimensional Effects." International Journal of Solids and Structures, Vol. 22, pp. 121-138.

Rousseau, C.-E., 2000, "Evaluation of Crack Tip Fields and Fracture Parameters in Functionally Graded Materials." Ph.D. Dissertation, Auburn University.

Rousseau, C.-E., and Tippur, H. V., 2000, "Compositionally Graded Materials with Cracks Normal to the Elastic Gradient: Examination of Fracture Parameters Relative to Bimaterials." Acta Materialia, Vol. 48, pp. 4021-4033.

Sinha, J. K., Tippur, H. V., and Xu, L., 1997, "An Interferometric and Finite Element Investigation of Interfacial Crack Tip Fields: Role of Mode-Mixity on 3-D Stress Variations." International Journal of Solids and Structures, Vol. 34, No. (6), 741-754.

Tippur, H. V., Krishnaswamy, S., and Rosakis, A. J., 1991, "A Coherent Gradient Sensor for Crack Tip Deformation Measurements: Analysis and Experimental Results." International Journal of Fracture, Vol. 48, pp. 193-204.

Weng, G. J., 1984, "Some Elastic Properties of Reinforced Solids, with Special Reference to Isotropic Ones containing Spherical Inclusions." International Journal of Engineering Science, Vol. 22, pp. 845-856.

Table 1. Comparison of computed and measured SIFs for a far-field bending stress $(6M / BW^2) = 10.2$ MPa.

| Method of calculation | FGM $E_2 / E_1 = 2.23$ $E_0 = 4.8$ GPa | Homogeneous $E_2 / E_1 = 1$ $E_0 = 4.8$ GPa | FGM $E_2 / E_1 = 0.41$ $E_0 = 6.8$ GPa | Homogeneous $E_2 / E_1 = 1$ $E_0 = 6.8$ GPa |
|---|---|---|---|---|
| FEA (Plane stress) | 1.27 | 1.51 | 1.77 | 1.45 |
| Optically Measured ($K$-dominant description) | 1.06 | 1.26 | 1.44 | 1.20 |
| Optically Measured (Asymptotic expansion) | 1.13 | 1.44 | 1.80 | 1.50 |

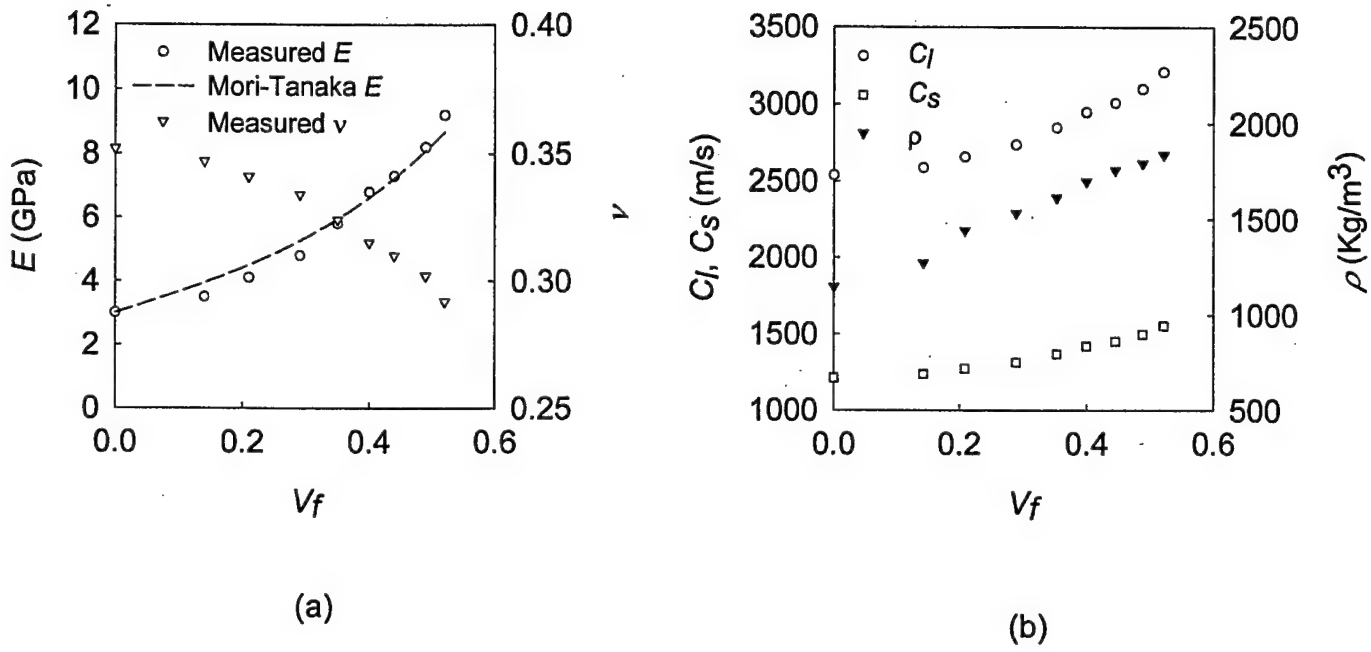


Figure 1. Material properties of glass-filled epox particulate composites.
a) Static Young's modulus and Poisson's ratio with filler volume fraction.
b) Wave speeds and density with filler volume fraction.

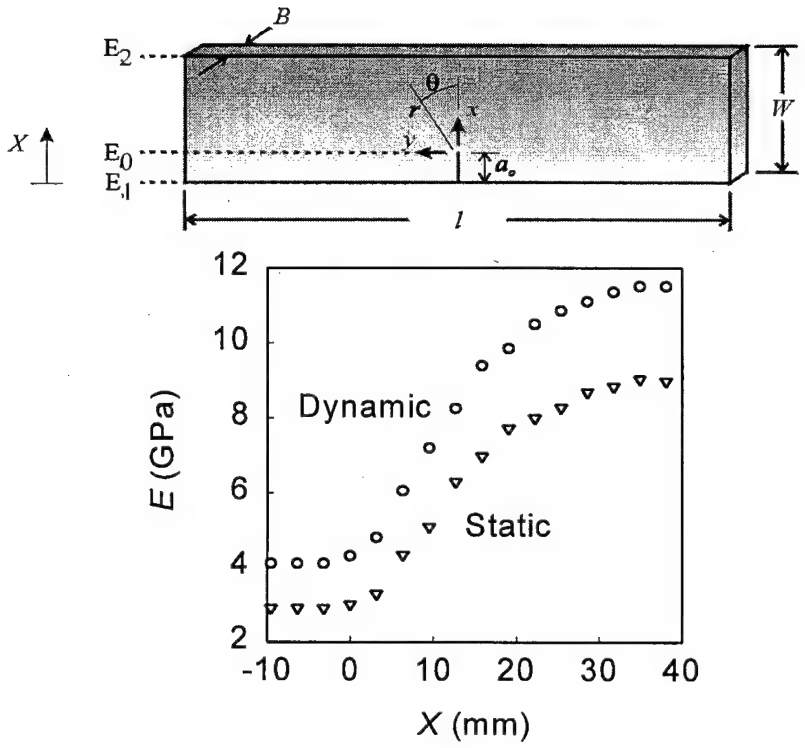


Figure 2. Typical Young's modulus variations in FGM plates.

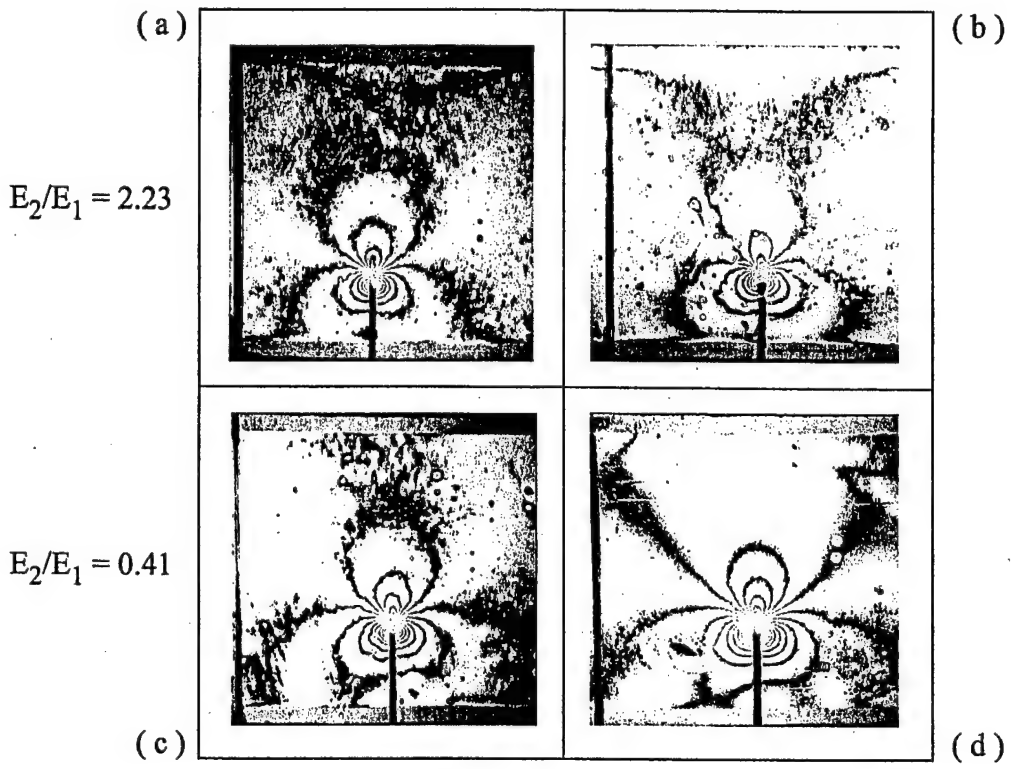


Figure 3. Crack tip interference patterns representing $\delta w / \delta x$ contours for a far-field bending stress $(6M / BW^2) = 10.2$ MPa: a) FGM with $E_2 / E_1 = 0.41$, b) homogeneous counterpart of (a), c) FGM with $E_2 / E_1 = 2.23$, d) homogeneous counterpart of (c), (center to center distance from crack to drawn line is approximately 10 mm).

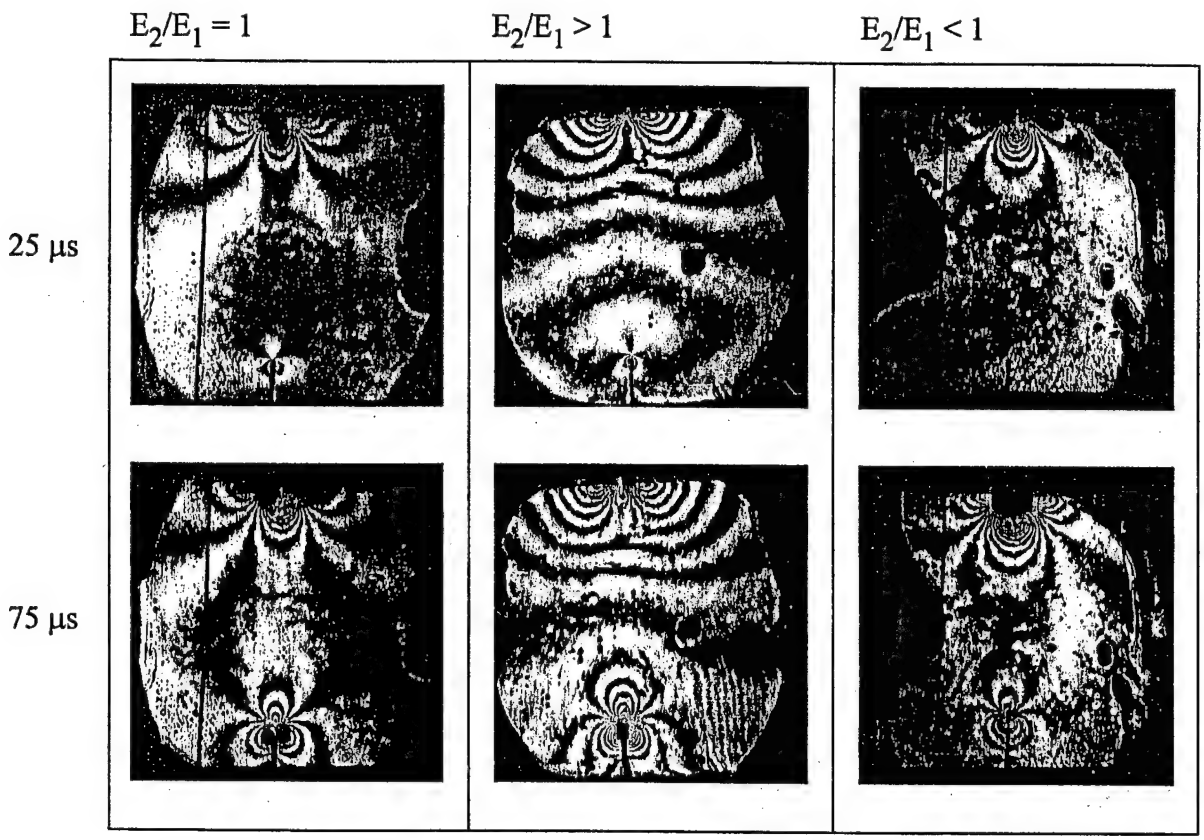


Figure 4. Representative crack tip interference representing surface slope $\delta w / \delta x$ contours for homogeneous and FGM samples (fringe sensitivity 0.015°/fringe).

| | STATIC FEA | DYNAMIC FEA |
|---|---|---|
| ***B*** | 6 mm | 6 mm |
| ***W*** | 20 mm | 37 mm |
| ***L*** | 150 mm | 120 mm |
| ***l*** | 60 mm | - |
| ***a*** | 6 mm | 6 mm |
| | At C, H support and loading boundary conditions prescribed | At D velocity boundary condition prescribed |

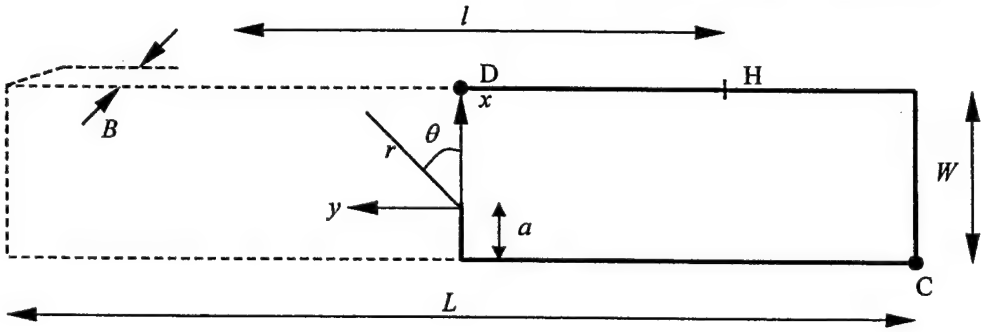


Figure 5(a): Schematic of geometry and loading configuration used in FEA.

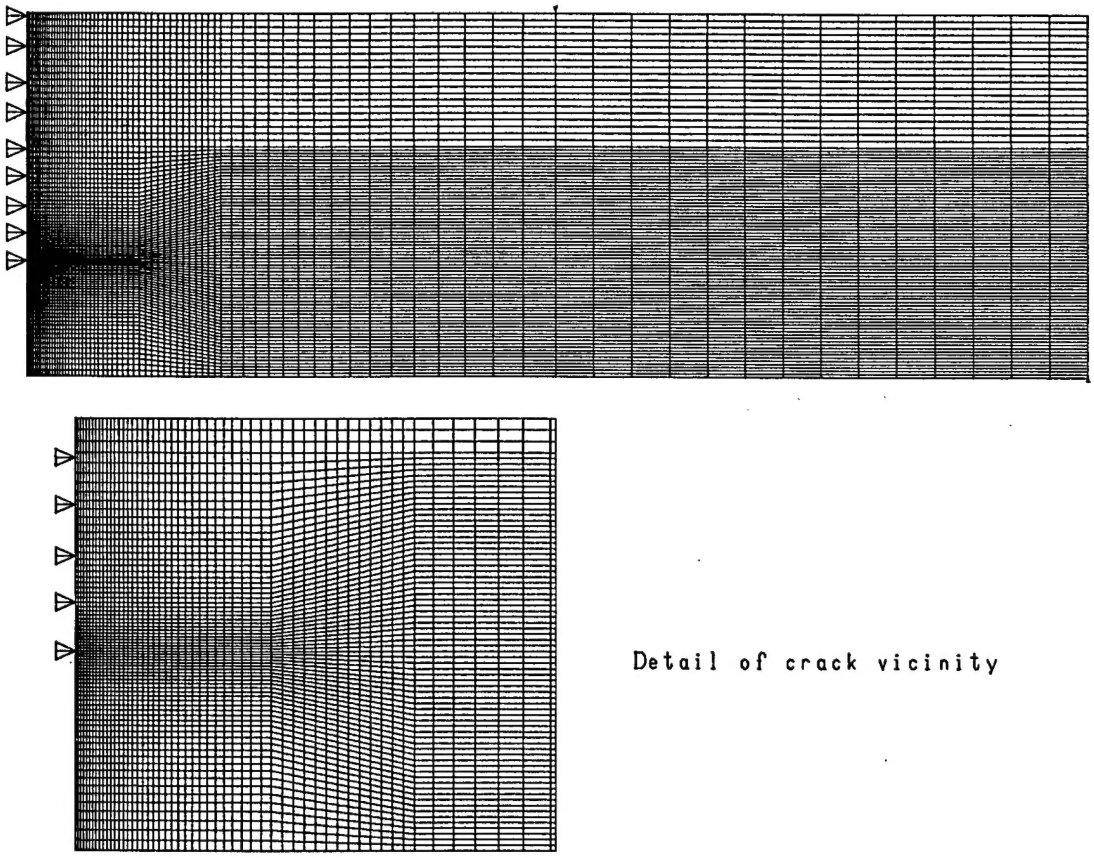


Figure 5*b*.Typical finite element mesh.

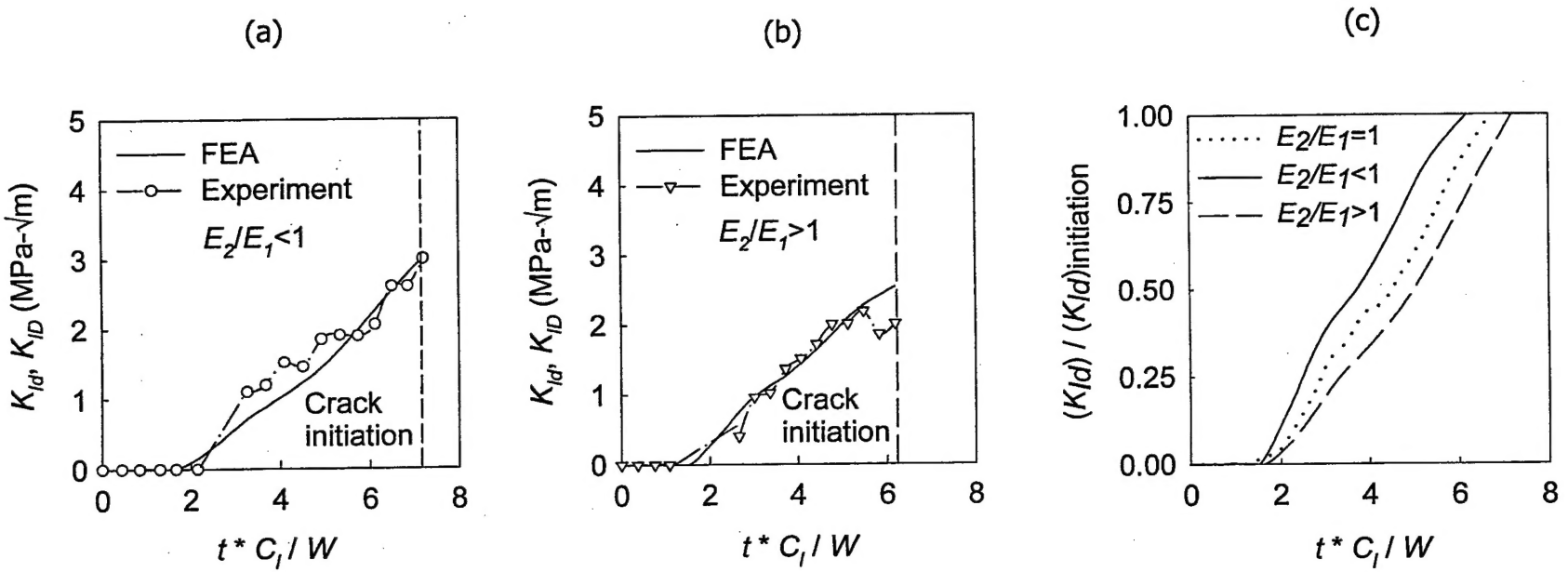


Figure 6. Apparent mode-I dynamic stress intensity factor history for FGM with $E_2 / E_1 < 1$ (a), and $E_2 / E_1 > 1$ (b). Normalized SIF for FGMs and homogeneous material (c).

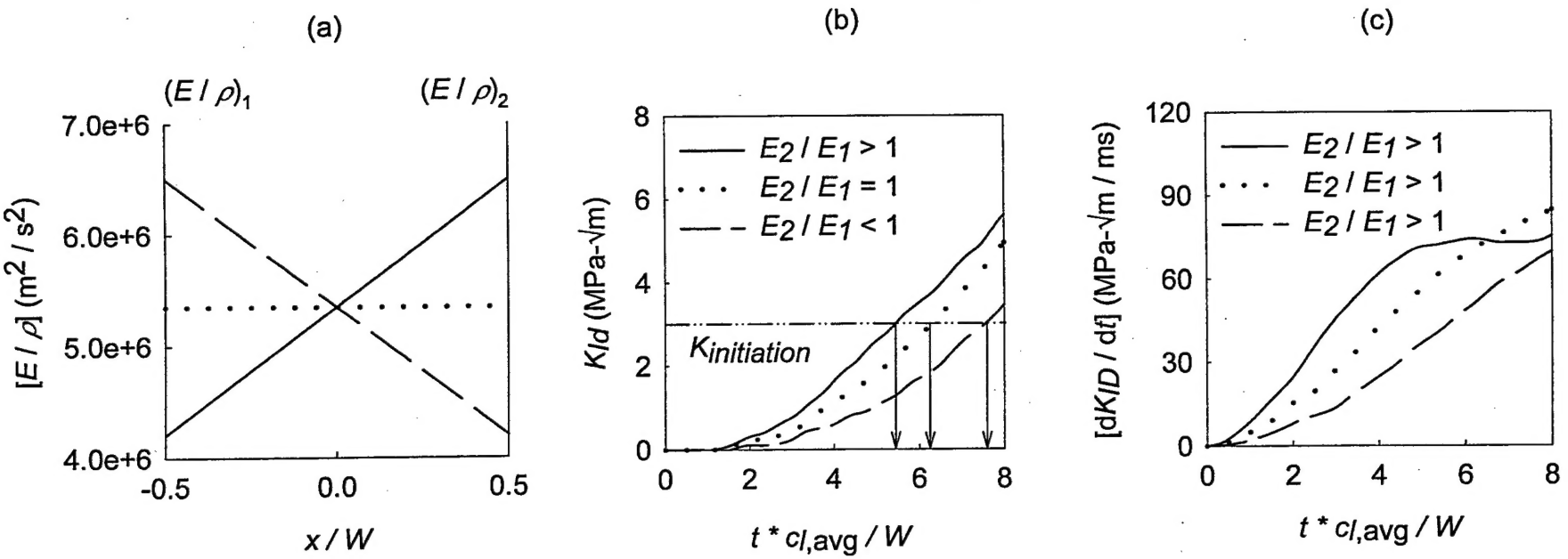


Figure 7. Stress intensity factor history in homogeneous beams and FGMs with linearly varying gradients (crack tip located at $X/W = 0.5$ or $x/W = 0$).

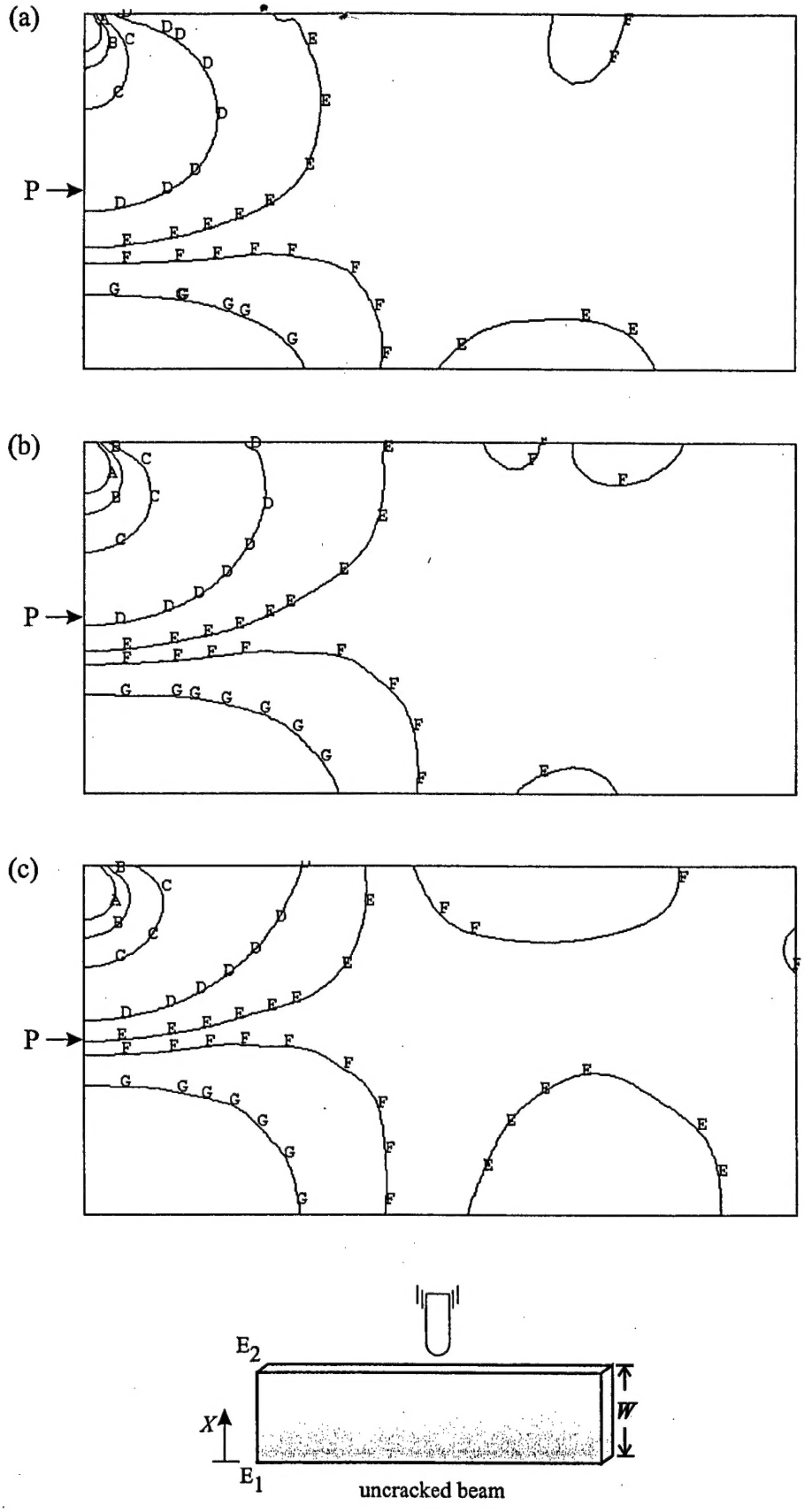


Figure 8. ($\sigma_x + \sigma_y$) contours at non-dimensional time $T = 5.7$. (A = -5, B = -3.5, C = -2, D = -0.5, E = -0.1, F = 0.1, G = 0.5) * 10 MPa. a) $E_2 / E_1 < 1$, b) $E_2 / E_1 = 1$, c) $E_2 / E_1 > 1$. Point P corresponds to ($X / W = 0.5, y = 0$). Note that only half of the beam is modeled.